

Design and Synthesis of Intramolecular Ion-Pairing *cis*-Bicyclo[4.4.0]decane (*cis*-Decalin) Amino Acids: Conformation-Based Probes of Electrostatic Interactions in Water

Craig Beeson[†] and Thomas A. Dix^{*†‡}

Departments of Chemistry and Biological Chemistry, The University of California, Irvine, California 92717

Received December 18, 1991

The design strategy and synthesis of *cis*-bicyclo[4.4.0]decane (*cis*-decalin) derivatives as conformation-based probes of electrostatic interactions in H₂O are described. The molecules were designed so that formation of an intramolecular electrostatic interaction occurs in only one of two low-energy conformers; hence, the conformational equilibrium of a given molecule is under control of the electrostatic interaction, which can be determined accurately with NMR studies. The structural definition inherent to the molecules will enable the thermodynamics and kinetics of solvent reorganization, which controls formation of electrostatic interactions in H₂O, to be probed directly. The first probe, a *cis*-decalin amino acid designed to evaluate an intramolecular ion pair, has been synthesized. The total synthesis was efficient and illustrated many of the strategies and potential pitfalls associated with the preparation of conformationally flexible ring systems. In particular, the inherent facial selectivity afforded by the shape of the *cis*-decalin, a critical component of the synthetic design, was reversed in one step in which hydrogen was added from the sterically encumbered concave face of the molecule. A *cis*-decalin amino acid of a different stereoelectronic array was also prepared. These molecules are the first examples to emerge from the application of a general design and synthetic strategy that will enable probes for all of the important biological electrostatic interactions to be constructed. The study of these molecules will provide significant insight into the synergistic role of molecular structure and solvent at controlling electrostatic interactions in H₂O, an important basis of biological structure and function.

Introduction

Electrostatic interactions are central to biomolecular structure and functioning.¹ Despite the importance, an adequate understanding of the control of biologically significant electrostatics at the level of the individual interactions is lacking, which has significant theoretical and practical consequences. Theoretically, a precise, quantitative, definition of individual electrostatic interactions is needed for a complete description of important biological processes such as protein folding, enzyme-substrate binding and catalysis, and protein-DNA interactions. From a practical point of view, the ability to rationally (re)design biologically active agents such as drugs and peptide hormones would be improved greatly if electrostatic binding to the appropriate biological targets could be modulated in a predictable fashion. One key factor inhibiting progress in this area results from the difficulty in studying individual interactions in the context of the structural complexity of large biomolecules. Often, changes made to evaluate one type of interaction (for example, the site-specific mutagenesis of a particular amino acid residue of a protein) often influence the overall structural integrity of the molecule in ways that are difficult to evaluate or detect.² Furthermore, the need to evaluate solute induced perturbations of the potential and kinetic energy of solvent molecules in a description of solution equilibria³ has been well recognized but difficult to implement.^{4,5}

Models of ionic solvation, which are now quite reliable for calculation of solvation free energies, have described the roles of solvent dipoles, polarization, and van der Waals interactions in ion stabilization.^{1a} The free energies of ion solvation are dominated by the enthalpy terms; for example, ΔH and $T\Delta S$ for solvation of inorganic anions and cations average -110 kcal mol⁻¹ and -8 kcal mol⁻¹, respectively.⁶ However, during the formation of electrostatic interactions, enthalpic or entropic changes may dominate. Calculation of the free energies of formation of methyl

ammonium acetate and glycine zwitterion from neutral species suggest that the entropy terms dominate the differences in observed free energies.⁷ The significant differences in entropies of ionization between substituted carboxylic acids, such as trichloroacetic and acetic acid, are commonly attributed to changes in solvent reorganization in response to the different charge densities.^{8,9} Recent experimental results also suggest that formation of a hydrogen bond in water may be driven primarily by entropy changes.^{5b} In the context of protein electrostatic interactions, however, the relative importance of the ΔH and $T\Delta S$ terms should vary dramatically. The protein "solvent" interior includes fixed and induced dipoles and van der Waals interactions only,^{1a} which are unable to adapt to structural changes to the same degree as would

(1) Electrostatics in biology: (a) Warshel, A.; Russell, S. T. *Q. Rev. Biophys.* 1984, 17, 283. (b) Warshel, A. *Acc. Chem. Res.* 1981, 14, 284. (c) Anderson, C. F.; Record, M. T. *Ann. Rev. Biophys. Biophys. Chem.* 1989, 19, 423. (d) Sharp, K. A.; Honig, B. *Ann. Rev. Biophys. Biophys. Chem.* 1990, 19, 301.

(2) Klotz, I. M. *Q. Rev. Biophys.* 1985, 18, 3.

(3) Hammett, L. P. *Physical Organic Chemistry*; McGraw-Hill: New York, 1940.

(4) Interaction of biomacromolecules with solvent water: (a) Kauzmann, W. *Adv. Prot. Chem.* 1959, 14, 1. (b) Kuntz, I. D., Jr.; Kauzmann, W. *Adv. Protein Chem.* 1974, 28, 239. (c) Franks, F. *Phil. Trans. R. Soc. London B* 1977, 278, 33. Edsall, J. T.; McKenzie, H. A. *Adv. Biophys.* 1978, 10, 137. (d) Edsall, J. T.; McKenzie, H. A. *Ibid.* 1983, 16, 53. (e) Eisenberg, D.; McLachlan, A. D. *Nature* 1986, 319, 199. (f) Gilson, M. K.; Honig, B. *Proteins: Str. Funct. Genet.* 1988, 4, 7. (g) Ben-Naim, A.; Ting, K. L.; Jernigan, R. L. *Biopolymers* 1990, 29, 901. (h) Livingstone, J. R.; Spolar, R. S.; Record, M. T. *Biochemistry*, 1991, 30, 4237.

(5) Recent molecular recognition studies that incorporates the role of solvent water: (a) Smithrud, D. P.; Wyman, T. B.; Diederich, F. *J. Am. Chem. Soc.* 1991, 113, 5420. (b) Williams, D. H., Cox, J. P. L.; Doig, A. J.; Gardner, M.; Gerhard, U.; Kaye, P. T.; Allick, A. R.; Nicholls, I. A.; Salter, C. J.; Mitchell, R. C. *J. Am. Chem. Soc.* 1991, 113, 7020. Cox, J. P. L.; Nicholls, I. A.; Williams, D. H. *J. Chem. Soc., Chem. Commun.* 1991, 1295.

(6) Krishnan, C. V.; Friedman, H. L. In *Solute-Solvent Interactions*; Coetzee, J. F., Ritchie, C. D., Eds.; Marcel-Dekker: New York, 1976; Vol. 2.

(7) Haberfield, P. In *Environmental Influences and Recognition in Enzyme Chemistry*; Liebman, J. F., Greenberg, A., Eds.; VCH: New York, 1986.

(8) March, J. *Advanced Organic Chemistry*, 3rd ed.; Wiley & Sons: New York, 1985.

(9) Larson, J. W.; Hepler, J. G. In *Solute-Solvent Interactions*; Coetzee, J. F., Ritchie, C. D., Eds.; Marcel-Dekker: New York 1976; Vol. 1.

* To whom correspondence should be addressed at the Department of Chemistry.

[†] Department of Chemistry.

[‡] Department of Biological Chemistry.

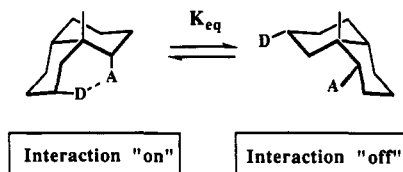


Figure 1. *cis*-Decalin low-energy conformers: the basis of probe design. D and A represent electrostatic donor/acceptor groups.

a solvent.¹⁰ Yet, a description of surface electrostatic interactions, conformational transitions, enzyme-substrate binding, or protein folding would include free energy changes due to solvent reorganization. Clearly, a precise definition of the relationship between H₂O structural changes and the ability of structurally defined molecules to generate electrostatic interactions, in loose analogy to studies of the H₂O-driven "hydrophobic effect",¹¹ would enhance our understanding of biological structure and function.

In this paper, we describe the conceptualization and design of *cis*-bicyclo[4.4.0]decane (*cis*-decalin) derivatives as molecular probes for solvation control of the thermodynamics of electrostatic interactions. The general design of our probes, as detailed in the first part of the paper, is presented in Figure 1. Each probe features electrostatic donor/acceptor (D/A) groups that can interact only in one of the two low-energy chair-chair conformers of the molecule. Accordingly, the observed conformational K_{eq} is the sum of the inherent steric bias of the ring (a constant) and the variable magnitude of the electrostatic interaction. The rigidly defined geometry between the interacting functional groups in each conformer removed structural uncertainties inherent in the formation of a biomolecular complex. This will permit the effects of solvent enthalpic and entropic perturbations on the free energy of the electrostatic interaction to be assayed directly. (The advantage of our approach is demonstrated in the Appendix in which the relative free energy changes associated with forming an intra- or intermolecular interaction, and the approximations attendant to both, are treated in detail.) The second part of this work describes the complete synthesis of the first probe: a *cis*-decalin amino acid whose analysis (¹H NMR) should prove useful in defining the changes in solvation energy associated with the formation of an ammonium-carboxylate ion pair. The generality of the synthesis can be applied directly to that of other *cis*-decalin-based probes. An unusual aspect of the synthesis was addition of hydrogen to a double bond from the concave face of the *cis*-decalin, a complete reversal of anticipated facial selectivity. Finally, the synthesis of a *cis*-decalin amino acid of a different stereoelectronic array and compounds whose conformational K_{eq} s are under control of both relative hydrophilic/hydrophobic surface area and/or intramolecular hydrogen bonds—the major elements controlling the definition of protein tertiary structure—are described.

Results

Structural Design. The *cis*-decalin bicyclic ring structure proved to be an ideal template for the design of intramolecular probes. The convex shape of the *cis*-decalin carbon skeleton, and its facile interconversion between

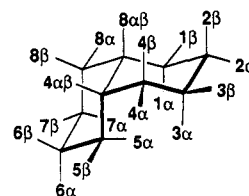


Figure 2. *cis*-Decalin substitution patterns.

low-energy chair-chair conformers,¹² permitted electrostatic donor and acceptor groups to be positioned such that they converge (adopt a favorable interaction geometry) in only one of the two conformers. Accordingly, the conformational K_{eq} of the molecule, as assayed by changes in ¹H-¹H NMR coupling constants, is under control of the electrostatic interaction. The exothermicity of the interaction could be counterbalanced with steric strain generated by the judicious placement of inert methyl groups; the magnitude of the strain could be estimated with molecular mechanics calculations.¹³ Molecular mechanics could also be used to predict the precise geometry of the interacting groups. This avoided the structural uncertainties inherent in bimolecular complex formation, which will permit direct assay of the crucially important solvent thermodynamic changes (see Appendix). The use of molecular mechanics also allowed for the screening of a large number of candidate molecules before synthesis of the best candidates was initiated; the fused bicyclohexane hydrocarbon ring system of the *cis*-decalin skeleton is the type of structure best evaluated by these calculations.^{13,14} Finally, the direct determination of the free energy of the electrostatic interaction, using changes in the molecule's ¹H-¹H coupling constants, will avoid the uncertainties inherent to the analysis of bimolecular complex formation. In particular, the indirect estimation of K_{eq} from chemical shifts does not always reflect correctly the populations of associated complexes.¹⁵

The large number of possible substitution patterns and subsequent interaction geometries inherent in *cis*-decalin conformers necessitated establishing a structural basis set on which to incorporate electrostatic donor-acceptor groups. We therefore initiated probe design with a systematic analysis of the relative geometries and conformational energies of all possible *cis*-decalin substitution patterns (Figure 2). As is obvious from the above discussion, only certain relative orientations of donor-acceptor groups will be appropriate for evaluating a given interaction; in addition, the inherent conformational bias of the molecule must be of the appropriate sign and magnitude to counterbalance formation of the interaction. Methyl groups were chosen for this analysis to mimic the steric bulk of possible donor-acceptor groups and to avoid the artificial incorporation of electrostatic interactions during molecular mechanics calculations. To generate the library of substitution patterns, a methyl group was placed on the first or second carbon adjacent to a bridgehead and a second methyl was placed on the other ring at the first or second carbon adjacent to the same or opposing bridgehead. In each case, four relative dispositions were generated in which the two methyls were *cis* ($\alpha\alpha$ and $\beta\beta$) or

(10) Hwang, J. K.; Warshel, A. *Nature* 1988, 334, 270.

(11) Muller, N. *Acc. Chem. Res.* 1990, 23, 23. Wood, R. H.; Thompson, P. T. *Proc. Natl. Acad. Sci. U.S.A.* 1990, 87, 946. Spolar, R. S.; Ha, J.; Record, M. T. *Proc. Natl. Acad. Sci., U.S.A.* 1989, 86, 8382. Privalov, P. L.; Gill, S. J. *Adv. Protein Chem.* 1988, 39, 191. Diederich and colleagues¹⁶ have recently studied the "hydrophobic effect" with host-guest molecules.

(12) Roberts, J. D.; Gerig, J. T. *J. Am. Chem. Soc.* 1966, 88, 2791.

(13) Lipkowitz, M. B.; Allinger, N. L. *QCPE Bulletin* 1987, 7, 19.

(14) (a) PCmodel (Clark Still, Columbia, running MMX). (b) Quanta (Polygen Corp., running CHARMM). (c) Semiempirical and ab initio calculations were performed using the SPARTAN package (Warren Hehre, UC-Irvine, not yet marketed).

(15) (a) Malecki, J. In *Molecular Interactions*; Ratajczak, H., Orville-Thomas, W. J., Eds.; Wiley: New York, 1983; Vol. 3. (b) Connors, K. A. *Binding Constants: The Measurement of Molecular Complex Stability*; Wiley: New York, 1987.

Table I. The Structural Library of *cis*-Decalin Dimethyl Derivatives with Their Predicted Conformational Energies

substituent pattern	C-C distance (Å) (conformation A) ^a	C-C distance (Å) (conformation B) ^b	ΔE_{MMX}^c (kcal/mol) ^c
1,1- <i>O</i> - α,α	3.3	5.4	-10.8
1,1- <i>O</i> - α,β	5.0	5.6	-4.8
1,1- <i>O</i> - β,β	6.1	4.9	1.2
1,1- <i>S</i> - α,β	4.6	3.2	-2.1
1,2- <i>O</i> - α,α	4.9	6.2	-1.2
1,2- <i>O</i> - α,β	5.4	6.8	6.9
1,2- <i>O</i> - β,β	6.0	6.8	-1.3
1,2- <i>O</i> - β,α	6.0	6.4	4.4
1,2- <i>S</i> - α,α	3.3	5.4	10.8
1,2- <i>S</i> - α,β	4.6	4.9	-3.2
1,2- <i>S</i> - β,β	5.0	5.4	2.5
1,2- <i>S</i> - β,α	3.9	6.4	-3.0
2,2- <i>O</i> - α,α	6.8	5.2	7.2
2,2- <i>O</i> - α,β	7.2	6.7	1.8
2,2- <i>O</i> - β,β	6.9	7.9	-3.7
2,2- <i>S</i> - α,β	7.0	6.0	5.6

^a Operationally defined as the indicated dimethyl derivative of the chair-chair conformer shown in Figure 2. ^b Operationally defined as the indicated dimethyl derivative of the chair-chair conformer not shown in Figure 2. ^c The difference between the minimized energies of the low energy conformers, as calculated for each conformer by molecular mechanics.^{14a}

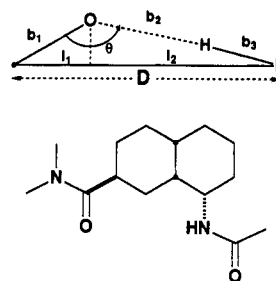
Table II. General Rules for Determining the Energy Cost of Axial Methyl Groups, as a Function of Position, for *cis*-Decalin Derivatives

substituent stereochem ^a	ΔE^b (kcal/mol)	bridgehead methyl same ^c (kcal/mol)	bridgehead methyl opposite ^d (kcal/mol)
1- β -axial	0.6	0.9	2.3
2- β -axial	1.8	2.5	0.4
1- α -axial	5.0	-0.7	0.2
2- α -axial	3.7	0.3	0.3

^a Relative to bridgehead. ^b Estimated energy for placing the methyl group in the indicated orientation. ^c Estimated energy cost of placing a methyl group in the indicated orientation on the same side of the ring as the bridgehead methyl group. ^d Estimated energy cost of placing a methyl group in the indicated orientation on the opposite side of the ring as the bridgehead methyl group.

trans ($\alpha\beta$ and $\beta\alpha$). An initial set of 24 conformations was reduced to 16 through symmetry analysis; for example, each chair-chair conformer of 1 α ,8 α -dimethylbicyclo[4.4.0]decane is the mirror image of the other, and hence useless for our application. For all unique conformational pairs, each conformation was energy minimized followed by determination of the dimethyl C-C distances and the differences in energy between the conformers. The data for all unique conformer pairs are listed in Table I, which constitutes the structural basis set on which to add electrostatic donor-acceptor groups. Appropriate distances between groups and the steric strain needed to balance out anticipated strengths of electrostatic interactions can be evaluated directly and quickly by inspection of the table.

The relatively simple, general, guidelines for determining the energy cost of axial methyl groups, as distinguished by their location at the first or second carbon adjacent to a bridgehead (1- or 2-axial), and by stereochemistry (α or β), are tabulated in Table II. As an internal check, estimated energies were quite consistent with values determined from molecular mechanics energy minimizations. For example, the conformational energy difference for *cis*-1 β ,3 α -dimethylbicyclo[4.4.0]decane was estimated by subtracting 0.6 kcal for the 1 β -axial methyl in the A conformation from 3.7 kcal for the 2 α -axial methyl in the B conformation (see Figure 2; the estimated value of 3.1 kcal compared favorably with the PCmodel^{14a} value of 3.2 kcal. The reproducibility of the energy estimates reflected the inherent simplicity of cyclohexane chair conformations and their applicability for analysis by molecular modelling,

**Figure 3. Candidate molecule for an amide-amide hydrogen bond gauge. The C=O_{carbonyl} N-H_{amide} bond geometry is shown above the molecule.**

which supported the initial rationale for choosing the *cis*-decalin ring system as the basic structure for the design of conformational probes.

The first evaluation of the design strategy was a conformational probe of the strength of an amide-NH amide-carbonyl hydrogen bond. To begin, the two methyl groups of a disubstituted *cis*-decalin were replaced with an amide NH donor and carbonyl acceptor; the geometric constraints of the hydrogen bond were used to identify those substitution patterns with an acceptable dimethyl C-C distance. Using the ideal amide H-O hydrogen bond distance of 1.9 Å¹⁶ and bond angle range of 160–180°,¹⁶ a dimethyl C-C distance range of 3.6–4.1 Å was determined. Examination of Table I identified one ideal candidate, the 1,2-*S*- $\beta\alpha$ substitution pattern, in which the two convergent methyl groups were separated by a distance of 3.9 Å. Accordingly, the donor and acceptor groups were placed in turn at the 1 position, with the other group occupying the 2 position, to give a total of two sets of conformer pairs for which to evaluate the geometric probability of forming an intramolecular hydrogen bond. Each diamide-substituted conformer was then computer minimized; an example of a molecule evaluated is shown in Figure 3. The computer modeling indicated that both substitution patterns produced pairs of conformers in which the donor-acceptor groups were in an favorable geometry to form an intramolecular hydrogen bond in one of the conformer pairs. To summarize the initial molecular evaluation, this approach permitted the rapid screening of 32 different structural motifs, which yielded two candidates for detailed evaluation of their conformational energies and synthetic accessibilities.

Two different force fields, MMX^{14a} and CHARMM,^{14b} were utilized during the above evaluation to avoid uncertainties unique to a single force field. For each molecule, torsions initially were manipulated to produce a hydrogen bond geometry, the molecule was energy minimized, and the energy of the minimized conformer was calculated in the absence of the explicit hydrogen bond imposed by the force field. To remove this interaction in the MMX force field, the hydrogen bond potential was removed explicitly; in the CHARMM force field, the gas-phase dielectric force field was replaced with a distance-dependent dielectric of 4, which mimicked an aqueous solution.^{14b} The MMX energy difference between the two conformations of the molecule illustrated in Figure 3 with and without the hydrogen bond interaction is -0.2 and 1.5 kcal, respectively, while the CHARMM energies are 0 and 3.4 kcal. The hydrogen bond geometries predicted by the two force fields were also different: the CHARMM force field gave a more idealized hydrogen bond geometry with a higher degree of torsional and angular deformation of the *cis*-decalin carbon skeleton.

(16) Baker, E. N.; Hubbard, R. E. *Prog. Biophys. Molec. Biol.* 1984, 44, 97.

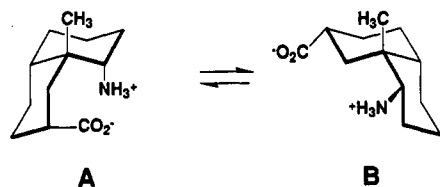


Figure 4. *cis*-Decalin probes for the free energy of an ammonium-carboxylate ion pair.

Table III. Predicted Steric Strain^a for *cis*-Decalin Ion-Pairing Probes 14a and 14b

calculn method	ΔE^b 14a (kcal/mol)	ΔE^b 14b (kcal/mol)
MMX	-4.6	-2.1
CHARMm	-9.3	-0.3
RHF/AM1	-3.1	0.5
RHF/3-21G*	-4.3	3.5

^a Steric energy difference for the neutral amino acids.

^b Calculated for the conformational equilibrium A \leftrightarrow B as defined in Figures 4 and 5.

Clearly, either one or both force fields did not evaluate correctly hydrogen bonding interactions, which further illustrated the need to synthesize and analyze molecular probes to calibrate the computations. At this point, it is uncertain which force field is more appropriate for this type of molecular design and analysis—both can be extremely useful tools as long as their limitations are understood and factored into the analysis.

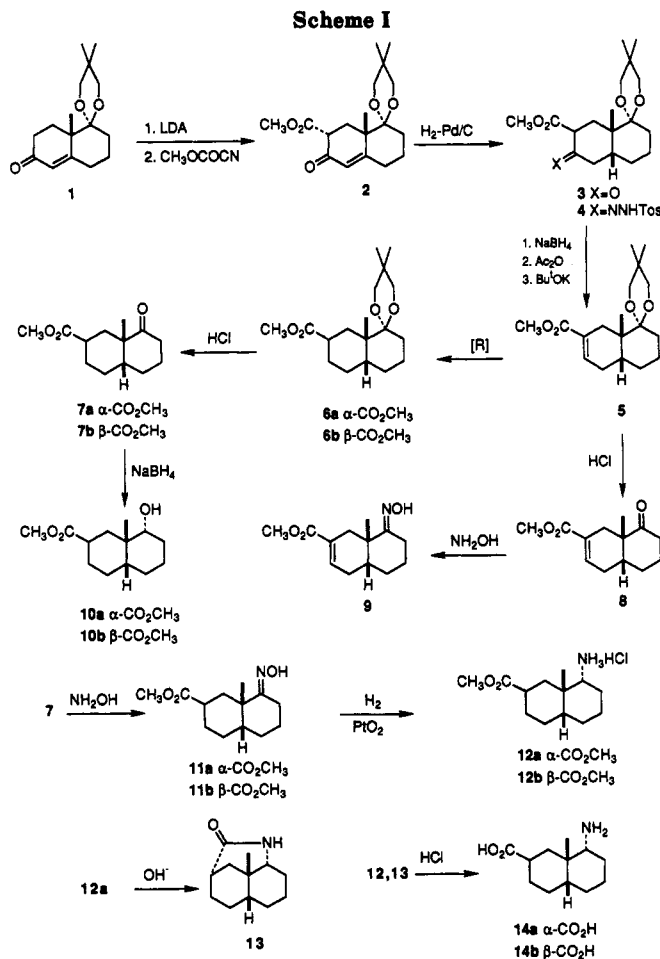
The identification of a *cis*-decalin dimethyl C-C distance acceptable for the generation of an intramolecular interaction did not always guarantee a satisfactory molecule. Even if a favorable relative orientation of the two substituents existed, the hydrogen-bonded rotamer could be a high energy rotamer. This was the case with the diamide probe prototype of Figure 3. The hydrogen-bonded rotamer for the bonding *cis*-decalin conformation; the difference in energy between it and a conformer in which the two carbonyls were antiparallel (the lowest energy conformer) was only 2.5 kcal (MMX), which is more consistent with the predicted value from Table I (3.1 kcal). While a satisfactory diamide probe did not result, the analysis demonstrated the utility of the approach in screening *cis*-decalin conformational probes and educated in potential pitfalls. Subsequent analyses, in which different amide donor/acceptor groups were removed in space from the *cis*-decalin skeleton with methylene linkers, eventually identified an appropriate amide hydrogen bond probe, whose synthesis and analysis will be described upon completion.

The design of a *cis*-decalin amino acid (Figure 4, 14a) to evaluate the energetics of ion-pairing directly paralleled that of the diamide as described above. However, the analysis immediately produced a satisfactory molecule, as the amide rotameric dispositions were eliminated by substitution of a rotationally symmetric ammonium ion and a less sterically demanding carboxylate ion. The resulting conformational probe, alternating between a contact and solvent separated ammonium-carboxylate ion pair (Figure 4), was produced by retaining the substitution pattern but changing the stereochemistry of the C7-carboxylate from β to α . Steric energies of 14a, as predicted by different molecular mechanics and ab initio packages, are summarized in Table III. Although the epimeric amino acid 14b was prepared for spectral comparisons, preliminary NMR analysis revealed that this compound was also capable of forming an intramolecular ion pair in certain solvents; it is thus an ion-pairing gauge of a different stereoelectronic

Table IV.

catalyst	H ₂ pressure (atm)	time (h)	% 6a:6b
10% Pd/C	3	12	<5:95 ^b
10% Pd/C	1	48 ^a	<5:95 ^b
PtO ₂	3	18	<5:95 ^b
5% Rh/Al ₂ O ₃	3	12	5:95
5% Rh/Al ₂ O ₃	1	48 ^a	5:95

^a Reaction went to 90% completion. ^b Resonances for 6a not observed in ¹H NMR spectra.



array than 14a. Since it will be studied further, its steric energies also appear in Table III.

Synthesis. The total synthesis of 14 is illustrated in Scheme I. Acylation of ketal 1 afforded β -keto ester 2 (90% yield); subsequent hydrogenation, which favors β addition of hydrogen,¹⁷ yielded *cis*-decalin 3 (80–90%) and the isomeric *trans*-decalin (10–15%). Although the ¹H NMR spectra of 3 was broadened by a slow ring puckering related to the enol-keto tautomerism, the ¹³C spectrum was nearly identical to that reported for the identical *cis*-decalin protected as an ethylene glycol ketal.¹⁸ In addition, a 4% NOE enhancement of the C4a bridgehead proton resonance was observed upon irradiation of the C8a angular methyl protons of 10a, and a low-temperature ¹H NMR of hydroxy ester 10b clearly permitted identification of the two *cis*-decalin chair-chair conformations. The highly enolic character of β -keto ester 3 (80% enol in CDCl₃ by NMR) complicated attempts to remove the

(17) Augustine, R. L.; Migliorini, D. C.; Foscante, R. E.; Sodano, C. S.; Sisbarro, M. J. *J. Org. Chem.* 1969, 34, 1075.

(18) Whitesell, J. K.; Minton, M. A. *Stereochemical Analysis of Allicyclic Compounds by C-13 NMR Spectroscopy*; Chapman and Hall: London, 1987.

C6-carbonyl without loss of stereochemical integrity. For example, reduction of tosylhydrazone 4 (NaBH_3CN , ZnCl_2) gave a 3:7 mixture of epimeric esters 6a and 6b (76% total yield). Alternatively, reduction of the ketone from the convex face and subsequent elimination to α,β -unsaturated ester 5 to regenerate the desired C7-stereochemistry was attempted. Sodium borohydride reduction of 3 (0 °C, MeOH), subsequent acetylation of the alcohol (Ac_2O , pyridine) and elimination (Bu^tOK , THF) gave alkene 5 in good overall yields (66% from 3). However, hydrogenation of 5 over 10% Pd/C (3 atm) produced ester 6b exclusively. Hydrogenation of 5 over a variety of other catalysts at different pressures also gave predominate or exclusive addition of hydrogen from the concave face of the *cis*-decalin.

The reversal of anticipated facial selectivity in the hydrogenation of 5 prompted an evaluation of the possible role of substituents in controlling addition stereochemistry. Hydrolysis of ketal 5 gave keto ester 8 (95% yield); again the hydrogenation stereoselectivity was unusual—hydrogenation of 8 over 5% Rh/ Al_2O_3 gave an optimal ratio of 30:70 for 7a:7b. Reduction of oxime 9 paralleled that of ketal 5 as hydrogenations over a variety of catalysts gave exclusively amino ester 12b. The reduction of 9 was particularly surprising—addition of hydrogen to C1, which is adjacent to a quaternary center, was exclusively from the convex face while addition to C6–C7 was exclusively from the concave face. The preference for hydrogen addition to the C6–C7 double bond from the concave face of the *cis*-decalin remains inexplicable: inspection of molecular models of alkenes 5, 8, and 9 suggested that the β face is less sterically encumbered, although the location of the double bond is somewhat removed from the steric bulk. A worst-case scenario might have predicted addition from both faces. This stereoselectivity was not restricted to hydrogenation reactions; reduction of alkene 5 with Mg in methanol, which was expected to add hydrogen from the convex face,¹⁹ also gave poor stereochemistry (95% yield of 6a:6b in a 3:7 ratio). This result might have been anticipated from the Mg reduction; an enolate intermediate can adopt a conformation with either an α - or β -carboxylate in an equatorial position, and addition of a less sterically discriminating proton from either face could scramble the stereochemistry. However, this was not the case: addition of water to the potassium enolate of 6 (KH, refluxing THF) followed the expected route to give 6a:6b in a 95:5 ratio (86% yield). For preparative purposes, the most efficient route to 6a proved to be hydrogenation of 5 and subsequent epimerization to give 6b (77% yield from 5, 51% yield from 3). The stereochemical assignments of 6a and 6b (and the keto esters 7a and 7b) were unambiguous; a NOE enhancement of the C8a angular methyl proton resonance was observed upon irradiation of the C7 proton (7% for 6a, 4% for 7a); a similar NOE was not observed from irradiation of the C7 proton of 6b or 7b.

Direct reductive aminations²⁰ (NH_4OAc or BnNH_2 , NaBH_3CN) of ketone 7a were unsatisfactory; typically, 7a was recovered with varying amounts (20–60%) of hydroxy ester 10a whose formation occurred during the acid quench. Hydroxy ester 10a existed solely in an intramolecular hydrogen bonded diaxial *cis*-decalin conformation in chloroform; thus, a different type of electrostatic probe was generated fortuitously. Ultimately, amino ester 12a was obtained from catalytic hydrogenation (3 atm, PtO_2)

of oxime 11a in glacial acetic acid (94% crude yield as acetate salt) although the isolation and purification of 12a proved troublesome. Conversion of the acetate of 12a to the free base produced only lactam 13 via a fast intramolecular ring closure ($t_{1/2}$, 5 min). The most efficient route to amino acid 14a was hydrolysis of lactam 13 (6 M HCl, 24 h, at 140 °C); the yields were quantitative. Spectral analyses of lactam 13 and amino acid 14a were unambiguous and consistent with the relative stereochemistry. Further confirmation of spectral assignments was obtained from analysis of the isomeric amino acid 14b which was prepared specifically for spectral comparisons; NOE data have the highest level of confidence only amongst a set of isomers.²¹ Formation of the lactam from 12a also provided chemical confirmation of the relative stereochemistry.

Discussion

Our approach to the design of conformation-based probes of electrostatic interactions is unique and has proven to be an efficient procedure for the identification of many different *cis*-decalin derivatives of interest whose preparations are currently in progress. Although the inherent structural simplicity, limited number of conformations, and convergent disposition of substituents initially dictated the choice of the *cis*-decalin bicyclic ring system as a template, our design strategy is not limited to any one structural motif. The simplicity of the energy rules given in Table II may also be applied to similar systems, for example, heterosubstituted *cis*-decalins and spiro[5.5]undecanes, with little modification. Thus, a large number of molecular geometries for the incorporation of electrostatic donor–acceptor groups are accessible directly; the major consideration for candidate molecules becomes one of synthetic feasibility.

Molecular mechanics computations proved quite reliable qualitatively and somewhat reliable quantitatively as an engineering tool for the determination of molecular geometries; we have recognized the utility of comparing minimized energy terms obtained from different force fields. As an example, either the MMX^{14a} or CHARMM^{14b} force fields reproduced the experimentally determined²² conformational energetics of the hydroxy ester 10a, although each predicted the existence of a hydrogen bond (in the gas phase). The experimentally²² determined enthalpy of the hydrogen bond (3–5 kcal), suggestive of a reasonable hydrogen bond geometry, was predicted better with the CHARMM force field, which allowed for more deformation of the ring to accommodate the hydrogen bond. In contrast, the calculated torsional and angular energies appeared to be more reasonable in MMX—reality undoubtedly lies somewhere between the two. Ultimately, the preparation and conformational analysis of many different molecules, based on the considerations outlined in this paper, will provide useful data sets for incorporation into the different force fields. The lack of absolute dependability of the calculated energetics will make it necessary to establish intrinsic K_{eq} s for each molecule under conditions in which the electrostatic interaction can be quenched.

The facial selectivity of *cis*-decalins, illustrated in the synthesis of the amino acid 14a, also demonstrated its utility in the engineering of conformational probes. However, the steric congestion of the convex face proved to be a synthetic problem at times. In particular, the

(19) Hudlicky, T.; Natchus, M. G.; Sinai-Zingde, G. *J. Org. Chem.* 1987, 52, 4641.

(20) Borch, R. F.; Bernstein, M. D.; Durst, H. D. *J. Am. Chem. Soc.* 1971, 93, 2897.

(21) Derome, A. E. *Modern NMR Techniques for Chemistry Research*; Pergamon Press: Oxford, 1987.

(22) Beeson, C.; Dix, T. A. Unpublished results.

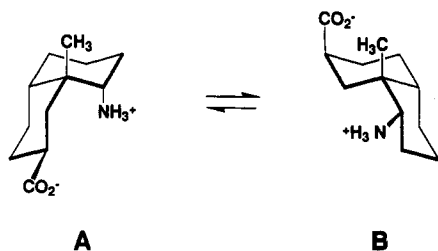


Figure 5. *cis*-Decalin probe for the free energy of a stereoelectronically poor ammonium-carboxylate ion pair.

presence of a quaternary center adjacent to the C1 ketone in **7** decreased substantially the *in situ* concentration of the imine intermediate during direct reductive aminations; a poor yield (<20%) of the benzyl imine of **7** under vigorous conditions (azeotropic removal of water in refluxing xylenes for 72 h) further attested to the added steric strain afforded by the convex face. The steric congestion was also reflected in the times required to reduce ketone **3** (4 h) and acetylate the resulting alcohol (5 days). The unexpected stereoselectivity of the hydrogenation of **5** serves as a warning against assumptions of facial selectivities and further exemplifies the need for a better understanding of the mechanism of heterogeneous catalytic hydrogenations.²³ The conformational flexibility also hampered spectral assignments; for example, both **7a** and **7b** adopt a chair-chair conformation with an equatorial carboxylate that produced nearly identical sets of proton resonances. Unambiguous assignments were possible only when ¹H-¹H connectivities and NOE enhancements were compared between isomers. Despite these complexities, the total synthesis was efficient: an overall yield of 36% of **14a** was obtained from **1**, and most of the reactions were not optimized rigorously.

At present, we are using *cis*-decalin amino acid **14a** to evaluate the energetics of ion-pairing in aqueous solutions; initial results have demonstrated that the molecule is performing as intended.²⁴ Molecule **14b** (Figure 5) also is capable of forming an intramolecular ion pair, which was surprising as the stereoelectronic disposition of the ions is poor. However, the free energy of ion-pairing as a function of stereoelectronics has not been explored experimentally—comparing the energetic behavior of **14a** and **14b** will thus be of great interest as ion pairs in proteins, for example, can have a variety of different relative orientations.²⁵ The fortuitous synthesis of hydroxy esters **10a** and **10b** provided molecules with which to characterize the energetics of formation of a hydrogen bond in aqueous solvents and the role of changes in solvent-accessible hydrophilic and hydrophobic surface area in controlling the interactions.²² These molecules thus mimic a protein as their conformational preferences are under control of the same factors—hydrophobicity and electrostatics—that control protein tertiary structure. Detailed NMR studies of the behavior of the molecules described in this paper will be reported in due time.

Experimental Section

General. For a standard workup the reaction mixture was extracted with ether (×3); the combined ether extracts were dried (MgSO₄) and evaporated on a rotary evaporator. Residues to be triturated were also evaporated at 0.1 mmHg. Tetrahydrofuran (THF) was distilled from the sodium benzophenone ketyl. Silica gel 60, 230–400 mesh, and 10% ethyl acetate in hexanes was used

for all chromatography unless stated otherwise.

Methyl 1,1-[(2,2-Dimethylpropane-1,3-diyl)dioxy]-6-oxo-8a-methyl-Δ^{4a,5}-octalin-7-carboxylate (2). A solution of ketal²⁶ **1** (9.5 g, 36 mmol) in 40 mL of THF was added dropwise to a stirred solution of LDA (42 mmol) in 20 mL of THF at -78 °C over 15 min; the resulting solution was stirred at 0 °C for 1 h and then cooled to -78 °C. HMPA (6.8 mL, 38 mmol) and methyl cyanofornate (3.6 mL, 45 mmol) were added rapidly, and the dry ice bath was removed. After 15 min the reaction was diluted with brine; workup provided a yellow solid which was triturated with 50 mL of cold ether and filtered giving 7.2 g (62% yield) of **2** as a white solid. Recrystallization of the filtrate gave another 3.2 g (28% yield) of **2**: ¹H NMR (500 MHz, CDCl₃) δ 5.80 (d, 1 H, *J* = 2.0 Hz), 3.77 (s, 1 H), 3.72 (d, 1 H, *J* = 11.2 Hz), 3.56 (d, 1 H, *J* = 11.2 Hz), 3.44 (dd, 1 H, *J* = 4.7, 15.2 Hz), 3.34 (dt, 2 H, *J* = 2.4, 11.2 Hz), 3.12 (t, 1 H, *J* = 14.4 Hz), 2.67 (m, 1 H), 2.40 (m, 1 H), 2.29 (m, 1 H), 2.06 (dd, 1 H, *J* = 4.7, 13.5 Hz), 1.72 (m, 1 H), 1.51 (m, 2 H), 1.30 (s, 3 H), 1.17 (s, 3 H), 0.72 (s, 3 H); ¹³C NMR (125 MHz, CDCl₃) δ 193.5, 171.2, 168.4, 124.5, 100.1, 70.1, 69.7, 52.0, 50.4, 45.6, 31.2, 29.8, 29.5, 23.4, 22.1, 20.8, 20.2, 19.2; HRMS (EI) exact mass calcd for M⁺ C₁₈H₂₆O₅ 322.1780, found 322.1795.

Methyl 1,1-[(2,2-Dimethylpropane-1,3-diyl)dioxy]-6-oxo-8a-methyloctalin-7-carboxylate (3). A solution of enone **2** (2.0 g, 6.2 mmol) in 200 mL of methanol with 200 mg 10% Pd/C was hydrogenated at 400 Torr H₂ (total pressure = 760 Torr, P_{Ar} = 360 Torr) for 12 h. The solution was filtered, evaporated to 75 mL, and cooled at -20 °C. Filtration gave 1.4 g (70% yield) of **3** as a white solid; fractional recrystallization of the filtrate yielded another 0.35 g (17% yield) of **3** and 0.15 g (7.5% yield) of the *trans*-decalin: ¹H NMR (500 MHz, CDCl₃) δ 12.25 (s, 0.7 H), 3.73 (s, 3 H), 3.70 (d, 2 H, *J* = 11.2 Hz), 3.64 (d, 2 H, *J* = 11.2 Hz), 3.31 (d, 2 H, *J* = 12.0 Hz), 2.55 (m, 2 H), 2.31 (br d, 1 H, *J* = 13 Hz), 2.12 (br d, 1 H, *J* = 13 Hz), 1.89 (br d, 1 H, *J* = 14 Hz), 1.85 (m, 1 H), 1.56 (m, 1 H), 1.39–1.21 (m, 5 H), 1.19 (s, 3 H), 1.10 (s, 3 H), 0.72 (s, 3 H); ¹³C NMR (125 MHz, CDCl₃) δ 173.2, 170.0, 100.3, 94.6, 69.7, 69.4, 51.2, 41.1, 35.8, 32.7, 29.8, 28.7, 26.4, 23.4, 22.3, 21.2, 21.1, 17.7; HRMS (CI) exact mass calcd for MH⁺ C₁₈H₂₆O₅H⁺ 325.2015, found 325.1993.

Reductions of Methyl 1,1-[(2,2-Dimethylpropane-1,3-diyl)dioxy]-6-(tosylhydrazono)-8a-methyloctalin-7-carboxylate (4). A solution of keto ester **3** (1.2 g, 3.7 mmol) and tosylhydrazine (0.9 g, 5 mmol) in 30 mL ethanol was refluxed for 6 h. The solution was evaporated to a volume of 10 mL and cooled at 0 °C. Filtration gave 1.8 g of a slightly yellow solid which was recrystallized from ethanol to give 1.6 g (89% yield) of tosylhydrazone **4**: ¹H NMR (500 MHz, CDCl₃) δ 9.82 (s, 0.8 H), 7.75 (d, 2 H, *J* = 8.1 Hz), 7.33 (d, 2 H, *J* = 8.1 Hz), 6.10 (s, 1 H), 3.69 (d, 1 H, *J* = 11.5 Hz), 3.64 (s, 3 H), 3.69 (d, 1 H, *J* = 11.5 Hz), 3.30 (bd, 2 H, *J* = 11 Hz), 2.53 (d, 1 H, *J* = 8 Hz), 2.44 (s, 3 H), 2.42–2.09 (m, 3 H), 1.74–1.24 (m, 5 H), 1.18 (s, 3 H), 0.95 (s, 3 H), 0.71 (s, 3 H); ¹³C NMR (125 MHz, CDCl₃) δ 170.5, 156.6, 144.7, 133.6, 129.8, 128.2, 100.4, 92.6, 69.7, 69.3, 50.7, 40.6, 35.2, 29.8, 29.1, 28.4, 27.3, 21.5, 21.2, 21.0; HRMS (EI) exact mass calcd for M⁺ C₂₆H₃₆N₂O₆S 493.2372, found 493.2364. A solution of **4** (0.40 g, 0.81 mmol), ZnCl₂ (0.14 g, 1.0 mmol), and NaBH₃CN (7.5 mg, 1.2 mmol) in 25 mL of anhydrous methanol was refluxed under argon for 12 h. The solution was evaporated and taken up in 10 mL of 0.1 M EDTA; chromatography of the residue obtained from workup gave 80 mg of **6a** (32% yield) and 110 mg of **6b** (44% yield). Spectral data for **6** is provided below.

Methyl 1,1-[(2,2-Dimethylpropane-1,3-diyl)dioxy]-8a-methyl-Δ^{6,7}-octalin-7-carboxylate (5). NaBH₄ (300 mg, 7.5 mmol) was added to a stirred solution of keto ester **3** (2.2 g, 7.4 mmol) in 400 mL of anhydrous methanol at 0 °C. After 4 h, glacial acetic acid was added until the solution was acidic (pH 5–6); the solution was partially evaporated and diluted with brine. Chromatography of the residue obtained from workup gave 2.2 g (92% yield) of the alcohol as a white solid: ¹H NMR (500 MHz, CDCl₃) δ 4.23 (br s, 1 H), 3.71 (d, 1 H, *J* = 11.1 Hz), 3.69 (s, 3 H), 3.62 (d, 1 H, *J* = 11.1 Hz), 3.28 (dt, 2 H, *J* = 11.1, 2.5 Hz), 2.72 (dt, 1 H, *J* = 14.2, 3.4 Hz), 2.53 (m, 1 H), 2.20 (dq, 1 H, *J* = 4.7, 13.5 Hz), 2.03 (t, 1 H, *J* = 13.2 Hz), 1.82 (dt, 1 H, *J* = 14.6,

(23) Randall Lee, T.; Wierda, D. A.; Whitesides, G. M. *J. Am. Soc. Chem.* **1991**, *113*, 8745.

(24) Beeson, C.; Dix, T. A. Submitted to *J. Am. Chem. Soc.*

(25) Barlow, D. J.; Thornton, J. M. *J. Mol. Biol.* **1983**, *168*, 867.

(26) Gopalakrishnan, G.; Jayaraman, S.; Rajagopalan, K.; Swaminathan, S. *J. Chem. Soc., Chem. Commun.* **1983**, 797.

4.6 Hz), 1.65 (m, 3 H), 1.49 (m, 1 H), 1.42 (br d, 1 H, $J = 13$ Hz), 1.27 (m, 2 H), 1.19 (s, 6 H), 0.70 (s, 3 H); ^{13}C NMR (125 MHz, CDCl_3) δ 176.7, 100.3, 69.6, 69.1, 66.0, 51.6, 42.9, 36.4, 32.9, 29.7, 29.3, 24.3, 23.5, 22.3, 21.2, 20.9, 16.5; HRMS (EI) exact mass calcd for $\text{M}^+ \text{C}_{18}\text{H}_{30}\text{O}_6$ 326.2093, found 326.2102. An excess of acetic anhydride (10 mL) was added to a solution of the alcohol (2.2 g, 6.7 mmol) in 25 mL of dry pyridine, and the solution was stirred for 5 days. The solution was evaporated, and the residue was chromatographed giving 2.2 g (88% yield) of the acetate and 300 mg of a 50:50 mixture of acetate-alcohol: ^1H NMR (500 MHz, CDCl_3) δ 5.35 (br s, 1 H), 3.65 (d, 1 H, $J = 11.8$ Hz), 3.62 (s, 3 H), 3.61 (d, 1 H, $J = 11.8$ Hz), 3.27 (br d, 2 H, $J = 13$ Hz), 2.82 (dt, 1 H, $J = 13.2$, 4.0 Hz), 2.56 (br d, 1 H, $J = 13$ Hz), 2.02 (t, 1 H, $J = 13.8$ Hz), 1.98 (s, 3 H), 1.97–1.82 (m, 3 H), 1.65 (m, 3 H), 1.50 (m, 1 H), 1.38–1.21 (m, 4 H), 1.17 (s, 3 H), 1.15 (s, 3 H), 0.70 (s, 3 H); ^{13}C NMR (125 MHz, CDCl_3) δ 173.1, 169.9, 100.1, 69.5, 69.2, 69.1, 51.5, 42.3, 41.8, 36.0, 31.1, 29.7, 28.7, 23.6, 22.3, 21.3, 21.2, 20.8, 16.4; HRMS (EI) exact mass calcd for $\text{M}^+ \text{C}_{20}\text{H}_{32}\text{O}_6$ 368.2199, found 368.2176. Bu^+OK (610 mg, 5.4 mmol) was added to a stirred solution of the acetate (2.0 g, 5.4 mmol) in 75 mL of THF at 0 °C, and the solution was stirred at room temperature for 30 min. Chromatography (5% ethyl acetate in hexanes) of the residue obtained from workup gave 1.4 g of 5 (82% yield, 66% yield from 3): ^1H NMR (500 MHz, CDCl_3) δ 6.91 (bs, 1 H), 3.73 (s, 3 H), 3.71 (d, 1 H, $J = 11.3$ Hz), 3.65 (d, 1 H, $J = 11.3$ Hz), 3.33 (dt, 2 H, $J = 11.3$, 2.4 Hz), 2.57 (dd, 1 H, $J = 9.2$, 3.1 Hz), 2.40 (m, 1 H), 2.27 (bd, 1 H, $J = 9$ Hz), 2.17 (dd, 1 H, $J = 9.3$, 2.2 Hz), 1.89 (m, 1 H), 1.74 (m, 1 H), 1.53 (m, 1 H), 1.19 (s, 3 H), 1.02 (s, 3 H), 0.72 (s, 3 H); ^{13}C NMR (125 MHz, CDCl_3) δ 168.8, 137.8, 128.3, 101.1, 70.4, 70.2, 52.1, 35.8, 30.8, 29.4, 28.9, 22.1, 22.0; HRMS (EI) exact mass calcd for $\text{M}^+ \text{C}_{18}\text{H}_{28}\text{O}_4$ 308.1987, found 308.1961.

1,4-Reductions of α,β -Unsaturated Ester 5. Hydrogenations. A solution of 5 (50 mg, 0.16 mmol) in 15 mL of methanol was hydrogenated at room temperature with 10% (w/w) of the indicated catalyst. After removal of the catalyst and evaporation, the product composition was determined from integration of the ^1H NMR. Ketals 6a and 6b were separated on silica with 5% ethyl acetate in hexanes.

Magnesium Reduction.¹⁹ Mg ribbon (100g, 1.52 mmol) was added to a solution of 5 (80 mg, 0.26 mmol) in 15 mL of anhydrous methanol under argon. A vigorous reaction ensued after 10 min; occasional immersion of the flask in an ice bath was required to temper the reaction. After complete dissolution of the Mg (3 h) the solution was acidified with dilute acetic acid; workup gave 73 mg of 6a:6b in a ratio of 25:75 (^1H NMR integration), respectively. **Epimerization of 12a.** KH (20 mg, 0.45 mmol) was added to a stirred solution of 6b (140 mg, 0.45 mmol) in 50 mL of THF. The solution was refluxed for 1 h, cooled to room temperature, and quenched with 10 mL of saturated $\text{NH}_4\text{Cl}_{(\text{aq})}$. Workup gave 120 mg of 6a:6b in a ratio of 95:5 (^1H NMR integration), respectively. Spectral data for 6a: ^1H NMR (500 MHz, CDCl_3) δ 3.69 (d, 1 H, $J = 13.8$ Hz), 3.64 (s, 3 H), 3.62 (d, 1 H, $J = 13.8$ Hz), 3.28 (dt, $J = 2.8$, 13.8 Hz), 2.60 (tt, 1 H, $J = 4.9$, 12.0 Hz), 2.53 (br d, 1 H, $J = 14$ Hz), 1.82–1.54 (m, 8 H), 1.41–1.22 (m, 4 H), 1.20 (s, 3 H), 1.18 (s, 3 H), 0.70 (s, 3 H); irradiation of H7 (δ 2.60) gives a 7% NOE enhancement of the C8a angular CH_3 resonance (δ 1.18); ^{13}C NMR (125 MHz, CDCl_3) δ 177.1, 100.4, 69.6, 69.2, 51.3, 42.4, 38.9, 36.5, 29.7, 29.2, 26.3, 26.2, 23.5, 22.6, 22.3, 21.2, 20.7, 16.9; HRMS (EI) exact mass calcd for $\text{M}^+ \text{C}_{18}\text{H}_{30}\text{O}_4$ 310.2144, found 310.2138. Spectral data for 6b (^1H and ^{13}C NMR spectra were extremely line broadened due to chemical exchange between the two chair–chair *cis*-decalin conformations): ^1H NMR (500 MHz, CDCl_3) δ 3.68 (d, 1 H, $J = 11.1$ Hz), 3.64 (s, 3 H), 3.59 (d, 1 H, $J = 11.1$ Hz), 3.25 (br, 1 H), 2.60–2.35 (br, 2 H), 2.00–1.75 (br, 3 H), 1.55–1.20 (br, 8 H), 1.18 (s, 3 H), 1.01 (s, 3 H), 0.69 (s, 3 H); HRMS (EI) exact mass calcd for $\text{M}^+ \text{C}_{18}\text{H}_{30}\text{O}_4$ 310.2144, found 310.2141.

Methyl 8a-Methyl-1-oxooctalin-7-carboxylate (7). A solution of ketal 6a (90 mg, 0.29 mmol) in 15 mL of methanol containing two drops of concd $\text{HCl}_{(\text{aq})}$ was stirred for 2 h and then evaporated. Chromatography of the residue obtained from workup gave 59 mg (91% yield) of keto ester 7a as a viscous oil: ^1H NMR (500 MHz, CDCl_3) δ 3.68 (s, 3 H), 2.57 (tt, 1 H, $J = 3.8$, 12.1 Hz), 2.30 (br d, 1 H, $J = 12$ Hz), 2.03 (m, 3 H), 1.81–1.53 (m, 8 H), 1.42 (dd, 1 H, $J = 4.2$, 12.2 Hz), 1.20 (s, 3 H); ^{13}C -NMR (125 MHz,

CDCl_3) δ 214.9, 175.9, 51.6, 48.7, 41.6, 38.4, 37.6, 32.6, 26.6, 26.4, 25.0, 23.4, 20.3; HRMS (EI) exact mass calcd for $\text{M}^+ \text{C}_{13}\text{H}_{20}\text{O}_3$ 224.1412, found 224.1407. Hydrolysis of 6b under identical conditions gave 7b: ^1H -NMR (500 MHz, CDCl_3) δ 3.68 (s, 3 H), 2.55 (m, 2 H), 2.42 (br d, 1 H, $J = 14$ Hz), 2.22 (m, 2 H), 2.03–1.71 (m, 5 H), 1.51–1.30 (m, 4 H), 1.27 (s, 3 H), 1.07 (t, 1 H, $J = 14.2$ Hz); ^{13}C -NMR (125 MHz, CDCl_3) δ 215.0, 176.2, 51.4, 49.1, 44.6, 39.4, 37.7, 36.5, 28.9, 28.1, 27.0, 25.9, 22.0; HRMS (EI) exact mass calcd for $\text{M}^+ \text{C}_{13}\text{H}_{20}\text{O}_3$ 224.1412, found 24.1407.

Methyl 8a-Methyl-1-oxo- $\Delta^{6,7}$ -octalin-7-carboxylate (8). Ketal 5 was deprotected as described for 6 giving 89% yield of the alkene 8: ^1H NMR (500 MHz, CDCl_3) δ 6.98 (t, 1 H, $J = 2.3$ Hz), 3.74 (s, 3 H), 2.62 (m, 2 H), 2.43 (dddd, 1 H, $J = 13.7$, 3.5, 3.0, 3.0 Hz), 2.35 (dt, 1 H, $J = 15.0$, 4.2 Hz), 2.13–2.00 (m, 3 H), 1.78 (m, 1 H), 1.75–1.58 (m, 3 H), 1.05 (s, 1 H); ^{13}C NMR (125 MHz, CDCl_3) δ 214.6, 172.6, 136.8, 131.3, 51.6, 47.5, 40.2, 37.0, 30.0, 29.1, 27.6, 25.0, 20.2; HRMS (EI) exact mass calcd for $\text{M}^+ \text{C}_{13}\text{H}_{18}\text{O}_3$ 222.1256, found 222.1316.

1,4-Reductions of Alkene 8. A solution of alkene 8 (50 mg, 0.22 mmol) in 15 mL of methanol was hydrogenated at 50 psi for 12 h. Upon removal of the catalyst and evaporation, integration of the ^1H NMR of the crude material gave the product compositions: 10% Pd/C 7a:7b = 25:75, 5% Rh/ Al_2O_3 7a:7b = 30:70, respectively. A solution of 8 (35 mg, 0.16 mmol) and hydroxylamine hydrochloride (30 mg, 0.43 mmol) in 2 mL of methanol/1 mL of pyridine was stirred for 6 h. Upon evaporation, the residue was triturated with CH_2Cl_2 (1 mL) and filtered; the filtrate was passed through a small plug of silica and evaporated to give 30 mg of crude oxime 9 that was used without further purification. A solution of 9 in 10 mL of glacial acetic acid was hydrogenated over PtO_2 (5 mg, 3 atm H_2) for 12 h; after removal of the catalyst and evaporation an ^1H NMR spectrum of the crude acetate salt (500 MHz, D_2O) revealed a product composition of 12a:12b = 5:95 (spectral data for 12 given below).

Methyl 8a-Methyl-1-hydroxyoctalin-7-carboxylate (10). NaBH_3CN (11 mg, 0.18 mmol) was added to a stirred solution of ketone 7a (40 mg, 0.18 mmol) and NH_4OAc (140 mg, 1.8 mmol) in 7 mL of anhydrous methanol. After 50 h the solution was acidified to pH 2 and then basified to pH 10. Chromatography (1% CH_3OH in CH_2Cl_2) of the residue obtained from workup gave 15 mg of 10a (38% yield) and 17 mg of 7a (42% yield). The alcohol 10a was also obtained directly from NaBH_4 reduction of the ketone 7a using the same procedure as for the reduction of 5: ^1H NMR (500 MHz, CDCl_3) δ 4.17 (b, 1 H), 3.68 (s, 3 H), 2.80 (b, 1 H), 2.04 (m, 1 H), 1.88 (m, 2 H), 1.80–1.18 (m, 11 H), 1.03 (s, 3 H); ^{13}C NMR (125 MHz, CDCl_3) δ 178.2, 51.3, 40.1, 39.7, 37.9, 37.8, 30.5, 27.0, 25.6, 25.2, 24.8, 14.5; HRMS (CI) exact mass calcd for $\text{NH}^+ \text{C}_{13}\text{H}_{20}\text{O}_3\text{H}^+$ 227.1647, found 227.1645. Reduction of 7b under identical conditions gave the alcohol 10b; both ^1H and ^{13}C NMR spectra were extremely line broadened at room temperature due to exchange between the two chair–chair conformations: ^1H NMR (500 MHz, CDCl_3) δ 3.48 (s, 3 H), 3.06 (br, 1 H), 1.78 (br, 2 H), 1.62–1.03 (br m, 12 H), 0.88 (br, 3 H); HRMS (CI) exact mass calcd for $\text{M}^+ \text{C}_{13}\text{H}_{20}\text{O}_3$ 226.1569, found 226.1568.

Methyl 8a-Methyl-1-(hydroxyimino)octalin-7-carboxylate (11). Hydroxylamine hydrochloride (0.10 g, 1.4 mmol) was added to a stirred solution of the keto ester 7a (0.15 g, 0.67 mmol) in 3 mL of methanol and 1 mL of pyridine. After 6 h the solution was evaporated and the residue was triturated with CH_2Cl_2 and filtered; the filtrate was passed through a small plug of silica and evaporated to give 155 mg (97% yield) of the oxime 11a as a white solid: ^1H NMR (500 MHz, CDCl_3) δ 3.65 (s, 3 H), 3.28 (br d, 1 H, $J = 12$ Hz), 2.63 (tt, 1 H, $J = 4.4$, 13.3 Hz), 2.03 (t, 1 H, $J = 12.2$ Hz), 1.95–1.82 (m, 5 H), 1.74 (m, 1 H), 1.66 (dq, 1 H, $J = 3.8$, 12.7 Hz), 1.53–1.30 (m, 4 H), 1.26 (s, 3 H); ^{13}C NMR (125 MHz, CDCl_3) δ 176.2, 165.6, 51.5, 40.7, 40.6, 38.9, 34.1, 27.0, 26.5, 24.5, 22.9, 21.4, 20.2; HRMS (EI) exact mass calcd for $\text{M}^+ \text{C}_{13}\text{H}_{21}\text{NO}_3$ 239.1521, found 239.1508. The epimeric oxime 11b was prepared in an analogous manner: ^1H NMR (500 MHz, CDCl_3) δ 3.63 (s, 3 H), 3.26 (dd, 1 H, $J = 15.3$, 5.1 Hz), 2.80 (tt, 1 H, $J = 12.1$, 3.5 Hz), 2.41 (dt, 1 H, $J = 13.4$, 2.8 Hz), 2.04 (tt, 1 H, $J = 13.4$, 4.5 Hz), 1.97 (m, 1 H), 1.84 (dt, 1 H, $J = 6.5$, 15.3 Hz), 1.70–1.50 (m, 4 H), 1.50–1.37 (m, 4 H), 1.23 (s, 3 H); ^{13}C NMR (125 MHz, CDCl_3) δ 176.6, 162.4, 51.5, 43.5, 40.9, 39.0, 37.9, 29.2, 28.5, 27.4, 26.2, 19.8, 19.7; HRMS (EI) exact mass calcd for $\text{MH}^+ \text{C}_{13}\text{H}_{21}\text{NO}_3\text{H}^+$ 240.1600, found 240.1589.

Methyl 8a-Methyl-1-aminoctalin-7-carboxylate (12). A solution of the oxime 11a (30 mg, 0.12 mmol) in 10 mL of glacial acetic acid with 5 mg of PtO₂ was hydrogenated (3 atm H₂) for 12 h. The solution was filtered and lyophilized; addition of concd HCl_(aq) (0.5 mL) to the residue and subsequent lyophilization gave 30 mg of the crude HCl salt 12a. For preparative purposes it was best to convert crude 12a to the lactam 13 which was easily purified and hydrolyzed to the amino acid 14a. Analytically pure 12a was obtained from methanolysis of 14a: a drop of thionyl chloride was added to a solution of 14a (5 mg, 24 μmol) in anhydrous methanol at 0 °C; after 1 h the solution was lyophilized to give 5 mg of 12a: ¹H NMR (500 MHz, D₂O) δ 3.68 (s, 3 H), 3.08 (dd, 1 H, *J* = 4.3, 12.5 Hz), 2.68 (tt, 1 H, *J* = 4.1, 14.0 Hz), 1.98–1.51 (m, 8 H), 1.47–1.30 (m, 5 H), 1.18 (s, 3 H); ¹³C NMR (125 MHz, CDCl₃) δ 178.2, 59.3, 51.0, 37.7, 37.1, 34.5, 24.8, 24.7, 24.4, 24.2, 22.3, 21.2; HRMS (EI) exact mass calcd for C₁₃H₂₃NO₂ (free base) 225.1730, found 225.1716. Conversion of 7b to the oxime 11b and subsequent hydrogenation under the conditions described above gave the epimeric amino ester 12b; passage of HCl_(g) through an ether solution of the free base and recrystallization of the precipitate (ethanol) gave 12b as a white powder (64% yield from 7b): ¹H NMR (500 MHz, D₂O) δ 3.72 (s, 3 H), 2.93 (dd, 1 H, *J* = 12.5, 4.3 Hz), 2.77 (t, 1 H, *J* = 3.1 Hz), 2.05 (dd, 1 H, *J* = 13.8, 6.8 Hz), 1.94 (tt, 1 H, *J* = 4.4, 14.3 Hz), 1.87–1.78 (m, 2 H), 1.70 (dd, 1 H, 13.8, 1.7 Hz), 1.59 (dq, 1 H, *J* = 3.8, 12.7 Hz), 1.39–1.29 (m, 3 H), 1.13 (s, 3 H); ¹³C NMR (125 MHz, D₂O) δ 178.0, 61.8, 50.9, 38.2, 35.0, 34.1, 24.6, 24.2, 24.1, 23.5, 21.8, 21.6, 17.6; HRMS (EI) exact mass calcd for C₁₃H₂₃NO₂ (free base) 225.1730, found 225.1743.

12-Methyl-10-oxo-9-azatricyclo[6.2.2.0^{4,12}]dodecane (13). The crude HCl salt 12a (30 mg, 0.12 mmol) was dissolved in 10% NaOH_(aq). Chromatography (CH₂Cl₂) of the residue obtained from workup gave 20 mg (83% yield from 11a) of lactam 13: ¹H NMR (500 MHz, CDCl₃) δ 5.65 (br s, 1 H), 3.24 (br s, 1 H), 2.58 (br s, 1 H), 2.03 (m, 2 H), 1.86–1.63 (m, 5 H), 1.60–1.26 (m, 6 H), 1.03 (s, 3 H); ¹³C NMR (125 MHz, CDCl₃) δ 175.6, 57.0, 40.3, 38.3, 38.0, 30.8, 29.3, 28.2, 26.3, 26.1, 24.7, 14.6; HRMS (CI) exact mass calcd for MH⁺ C₁₂H₁₉NOH⁺ 194.1545, found 194.1544.

8a-Methyl-1-aminoctalin-7-carboxylic Acid (14). A solution of 13 (10 mg, 50 μmol) in 1 mL of 6 M HCl_(aq) was heated at 140 °C in a sealed tube for 24 h. The solution was evaporated and the residue taken up in 1 mL of water which was subsequently neutralized to pH 7.0 with NaHCO₃, deionized with an ion retardation gel (Biorex MSZ 501D), and lyophilized to give 10 mg (92% yield) of amino acid 14a: ¹H NMR (500 MHz, D₂O) δ 3.03 (dd, 1 H, *J* = 4.4, 12.3 Hz), 2.42 (tt, 1 H, *J* = 4.1, 13.8 Hz), 1.92 (tt, 1 H, *J* = 3.9, 13.6 Hz), 1.83 (br d, 1 H, *J* = 14 Hz), 1.76 (t, 1 H, *J* = 14.1 Hz), 1.72–1.49 (m, 3 H), 1.46–1.31 (m, 3 H), 1.23 (dd, 1 H, *J* = 3.9, 13.6 Hz), 1.19 (s, 3 H); ¹³C NMR (125 MHz, D₂O) δ 165.8, 61.4, 42.7, 40.1, 36.7, 34.1, 28.0, 26.9, 26.6, 24.5, 24.3, 23.5; HRMS (CI) exact mass calcd for MH⁺ C₁₂H₂₁NO₂H⁺ 212.1650, found 212.1672. Hydrolysis of 12b (6 M HCl, 120 °C 12 h) gave 14b in a 90% yield after deionization as described above: ¹H NMR (500 MHz, D₂O) δ 2.96 (dd, 1 H, *J* = 4.3, 12.4 Hz), 2.87 (t, 1 H, *J* = 3.2 Hz), 2.07 (dd, 1 H, *J* = 13.8, 5.4 Hz), 1.98 (tt, 1 H, *J* = 4.3 Hz), 1.90–1.54 (m, 5 H), 1.46–1.24 (m, 4 H), 1.09 (s, 3 H); ¹³C NMR (125 MHz, D₂O) δ 166.81, 61.9, 53.1, 40.3, 36.94, 36.91, 36.3, 26.7, 25.6, 24.3, 23.9, 19.7; HRMS (EI) exact mass calcd for M⁺ C₁₂H₂₁NO₂ 211.1572, found 211.1565.

Appendix

An analysis is made of the potential advantage of using an intra- versus intermolecular probe for the determination of the solvation component of the free energy of an electrostatic interaction. With the aid of a thermodynamic cycle for the formation of a bimolecular donor-acceptor complex (Figure 6) it can be shown that:

$$\Delta G^f_{[DA(aq)]} - \Delta G^f_{[DA(g)]} = \Delta G^{s \rightarrow w}_{[DA]} - \Delta G^{s \rightarrow w}_{[D]} - \Delta G^{s \rightarrow w}_{[A]} \quad (1)$$

Equation 1 is intuitively obvious—the difference in free energy between formation of the complex in water and in the gas phase, the solvation effect, is the difference in solvation free energies between the product and reactants.

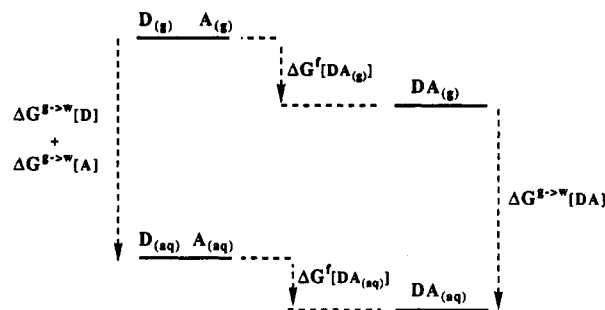


Figure 6. Thermodynamic cycle for determination of the solvation free energy of an electrostatic interaction. The free energy change for association of a donor and acceptor, $A + D \rightarrow DA$, is $\Delta G^f_{[DA]}$. The free energy change for transfer of a species from the gas phase to water, i.e., $D(g) \rightarrow D(aq)$, is $\Delta G^{s \rightarrow w}$.

Conceptually, one could measure the K_{eq} s for the aqueous and gaseous reactions to accurately calculate the solvation effect. However, the relative geometry of the biomolecular species DA is affected by the environment and the inherent “looseness” of the complex while that of an intramolecular DA interaction is not; thus, a bimolecular complex DA_(g) is unlikely to correspond to DA_(aq). At a more fundamental level, a bimolecular association in the gas phase incurs substantial losses in entropy (as much as $-55 \text{ cal mol}^{-1} \text{ K}^{-1}$)²⁷ while the diminished number of translational and rotational states available in solution results in less substantial entropy changes.²⁸ Although this is clearly a “solvation effect”, it is context-dependent and not intrinsic to the electrostatic interaction. Conversely, the major entropic contributions to an intermolecular process, translation and rotation, are essentially unchanged in an intramolecular process.

A more practical reference state, a hypothetical state of donor and acceptor at infinite separation in solution, has been developed for the estimation of free energies of simple ion pairs.^{1a} Although the infinitely separated reference state may not be applicable for an intramolecular process, an equally practical reference state would be the equivalent intramolecular process in which the electrostatic interaction is removed (i.e., neutral amino acid versus zwitterion). In a different approach, evaluations^{5b,29} of complex molecular assemblies stabilized by multiple interactions have largely depended on the conceptual free energy dissection initially described by Jencks.³⁰ In these evaluations, the intrinsic free energy of an electrostatic interaction within a bimolecular assembly is estimated from the observed free energy of association corrected for the reduction in translational/rotational entropy and for changes in free energy of solvation for those parts of the molecular assembly that do not actively participate in the interaction. However, these corrections are often substantial and rely on the premise of weak coupling between the various energy components—this may not always be valid for reactions in solution.³¹ The use of an intramolecular process to evaluate an electrostatic interaction eliminates, or substantially reduces, the need for such corrections, thus providing free energy values that should be more reliable. Finally, a practical difference between intra- and inter-

(27) Meot-Ner (Mautner), M.; Sieck, L. W. *J. Am. Chem. Soc.* 1983, 105, 2965.

(28) Doig, A. J.; Williams, D. H. *J. Am. Chem. Soc.* 1992, 114, 338.

(29) Fersht, A. R.; Shi, J.; Knill-Jones, J.; Lowe, D. M.; Wilkinson, A. J.; Blow, D. M.; Brick, P.; Carter, P.; Waye, M. M. Y.; Winter, G. *Nature* 1985, 314, 235. Kati, W. M.; Wolfenden, R. *Biochemistry* 1989, 28, 1919. Bartlett, P. A.; Marlowe, C. K. *Science* 1987, 235, 569.

(30) Jencks, W. P. *Proc. Natl. Acad. Sci., U.S.A.* 1981, 78, 4046.

(31) Nash, L. K. *Elements of Statistical Thermodynamics*, 2nd ed.; Addison-Wesley: Reading, 1974.

molecular processes arises from the method analysis—determination of K_{eq} for an intermolecular process often requires a concentration titration which, for a small K_{eq} , can be a substantial perturbation in the solvent composition. The analysis of an intramolecular process at a constant concentration precludes complications from changes in solvent activity.³²

Acknowledgment. We thank the donors of the Petroleum Research Fund, administered by the American

(32) Friedman, H. L.; Krishnan, C. V. In *Water*; Franks, F., Ed.; Plenum: New York, 1973; Vol. 3, Chapter 1.

Chemical Society (grant 21426-G4), and the University of California Cancer Coordination Research Committee for financial support of this research (to T.A.D.). C.B. is grateful for support as an National Institutes of Health predoctoral trainee (GM07311). The computer hardware was purchased with shared instrument funds from the National Institutes of Health (RR-05690) to T.A.D.

Supplementary Material Available: Proton NMR spectra for all characterized compounds (18 pages). This material is contained in many libraries on microfiche, immediately followed this article in the microfilm version of the journal, and can be ordered from the ACS; see any current masthead page for ordering information.

Use of *N*-Fmoc Amino Acid Chlorides and Activated 2-(Fluorenylmethoxy)-5(4*H*)-oxazolones in Solid-Phase Peptide Synthesis.¹ Efficient Syntheses of Highly *N*-Alkylated Cyclic Hexapeptide Oxytocin Antagonists Related to L-365,209[†]

Debra S. Perlow,* Jill M. Erb, Norman P. Gould, Roger D. Tung, Roger M. Freidinger, Peter D. Williams, and Daniel F. Veber

Department of Medicinal Chemistry, Merck Research Laboratories, West Point, Pennsylvania 19486

Received April 13, 1992

Fmoc amino acid chlorides have been shown to be useful reagents in the solid-phase synthesis of hexapeptides containing up to four sequential secondary amino acids. The oxytocin antagonist cyclo-(D-Phe-Ile-D-Pip-Pip-D-(*N*-Me)Phe-Pro) (1) was prepared in 70% overall yield starting from Boc-L-Pro-O-(PAM)-resin. In the synthesis of 1, the high reactivity of Fmoc-L-pipecolic acid chloride used in the di- to tripeptide step averted diketopiperazine formation seen with active ester couplings. The use of Fmoc-amino acid chlorides in the subsequent couplings provided a rapid method for assembly of the linear hexapeptide. The two potent cyclic hexapeptide oxytocin antagonists L-366,682 and L-366,948 were prepared in 45–48% overall yield on a 20 mmol scale using the methodology developed for the synthesis of 1. A particularly difficult coupling was encountered that involved acylation of a sterically hindered *N*³-Cbz-piperazic acid *N*-terminus with Fmoc-L-isoleucine. Excess Fmoc-L-isoleucine acid chloride in the presence of tertiary amine base gave only 30% conversion. The efficiency was improved to 76% by utilizing the acid chloride with AgCN in toluene. Further investigation revealed that this combination of reagents produces an activated form of the isoleucine 2-alkoxy-5(4*H*)-oxazolone derivative.

Introduction

Oxytocin (Figure 1) is a peptide hormone that plays a key role in the initiation and maintenance of uterine contractions associated with labor during pregnancy.² Recent evidence supports the concept of oxytocin receptor blockade as a new mechanism for treating preterm labor to prevent premature birth.³ The cyclic hexapeptide L-365,209 (Figure 1), a chemically modified derivative of a natural product isolated from *Streptomyces silvensis*, is a member of a structurally novel class of oxytocin antagonists⁴ and has served as the basis for a medicinal chemistry program aimed at improving its potency and aqueous solubility.^{5,6} L-365,209 is a cyclic peptide consisting of six amino acids of alternating configuration and containing an *N*-methylated phenylalanine at position 6 and the unusual amino acid, dehydropiperazic acid, at positions 4 and 5.⁷ We became interested in developing a solid-phase peptide synthesis method for the rapid production of L-365,209 analogs in order to define structure-activity relationships for this novel class of antagonist. The presence of four sequential secondary amino acids in

L-365,209 poses special problems. In particular, the slower rate of acylation of secondary amino acids requires special carboxyl group activation,⁸ and sequences of three or more secondary amino acids are known to be acid labile.⁹ These

(1) A portion of this work has appeared in preliminary form: Perlow, D. S.; Williams, P. D.; Tung, R. D.; Freidinger, R. M.; Chen, F. M. F.; Benoiton, N. L.; Veber, D. F. *Proceedings of the Twelfth American Peptide Symposium*; Smith, J. A., Rivier, J. E., Eds; ESCOM: Lieden, 1992; pp 564–565.

(2) Pritchard, J. A.; MacDonald, P. C.; Gant, N. F. *Williams Obstetrics*, 17th ed.; Appleton-Century Crofts: Norwalk, 1985; p 295.

(3) Anderson, L. F.; Lyndrup, J.; Akerlund, M.; Melin, P. *Am. J. Perinat.* 1989, 6, 196–199.

(4) Pettibone, D. J.; Clineschmidt, B. V.; Anderson, P. S.; Freidinger, R. M.; Lundell, G. F.; Koupal, L. R.; Schwartz, C. D.; Williamson, J. M.; Goetz, M. A.; Hensens, O. D.; Liesh, J. M.; Springer, J. P. *Endocrinology* 1989, 125, 217–222.

(5) Freidinger, R. M.; Williams, P. D.; Tung, R. D.; Bock, M. G.; Pettibone, D. J.; Clineschmidt, B. V.; DiPardo, R. M.; Erb, J. M.; Garsky, V. M.; Gould, N. P.; Kaufman, M. J.; Lundell, G. F.; Perlow, D. S.; Whitter, W. L.; Veber, D. F. *J. Med. Chem.* 1990, 33, 1843–1845.

(6) Bock, M. G.; DiPardo, R. M.; Williams, P. D.; Pettibone, D. J.; Clineschmidt, B. V.; Ball, R. G.; Veber, D. F.; Freidinger, R. M. *J. Med. Chem.* 1990, 33, 2321–2323.

(7) The amino acids in L-365,209 and its analogs are numbered to reflect the structural homology of the D-Phe-Ile dipeptide in L-365,209 with the Tyr²-Ile³ dipeptide moiety found in oxytocin.

(8) Tung, R. D.; Rich, D. H. *J. Am. Chem. Soc.* 1985, 107, 4342–4343.

(9) Anteunis, M. J. O.; Van Der Auwera, C. *Int. J. Pept. Prot. Res.* 1988, 31, 301–310.

[†] Dedicated to Professor Ralph F. Hirschmann on the occasion of his 70th birthday.